INTEGRATOR RESET ANTI-SPIN FOR MARINE THRUSTERS OPERATING IN FOUR-QUADRANTS AND EXTREME SEA CONDITIONS

Jostein Bakkeheim * **Luca Pivano** * **Tor A. Johansen** *
Øyvind N. Smogeli **

* *Department of Engineering Cybernetics, Norwegian University of Science and Technology, Trondheim, Norway*
** *Marine Cybernetics, Vestre Rosten 77, NO-7075 Tiller, Norway*

Abstract: Transient regimes arise when the propeller of a ship is operating in extreme seas, where ventilation and in-and-out of water effects results in loss of propeller thrust. By introducing Lyapunov based controller state reset, the performance in transient regimes may be increased without influencing the performance in calm seas. Improvements have been presented previously for dynamically positioned (DP) vessels. Transit operations, however, introduces additional losses due to variations in the propeller advance velocity. The controller in this paper combines an existing shaft speed reference generator that uses an estimate of the propeller torque losses with a PI shaft speed control law with integrator reset. Moreover, an anti-spin strategy is included to be able to operate also in extreme seas. The method is experimentally validated in a towing tank.

Keywords: Switching algorithms, Lyapunov function, Marine systems, Anti-spin regulation, PI controllers, Propulsion control

1. INTRODUCTION

The control hierarchy of marine vessels with electrically driven thrusters consists of a high-level controller giving commands to a thrust allocation scheme. The thrust allocation scheme gives in turn commanded set-points to the different local thruster controllers (LTC), see Sørensen (2005). Dynamic positioning (DP) systems, joysticks, and autopilots are examples of high-level controllers, widely covered in the literature. In the last years also LTC has gained growing interest in the literature see Smogeli (2006), Whitcomb and Yoerger (1999), Pivano et al. (2007), Bakkeheim et al. (2006) and the references therein.

Today's industrial standard for fixed pitch propellers is proportional and integral (PI) controllers on the propeller shaft speed. These controllers are usually tuned in such a way that the performance is maximized when operating in calm or moderate seas. In extreme seas where ventilation and in-and-out of water effects may occur, the controller may give poor performance due to shaft load variations. This, in turn, may lead to wear and tear of the mechanical parts of the propulsion system, and undesired transients on the power network that may increase the risk of blackouts due to overloading of the generator sets, see Radan et al. (2006).

Different anti-spin strategies have been introduced in order to handle these phenomena, see Smogeli et al. (2004), Bakkeheim et al. (2006) and Smogeli (2006). These controllers utilize an estimate of the torque loss to detect ventilation incidents. The anti-spin controller in Smogeli et al. (2004) is based on a combined power/torque controller which in order takes control of the propeller shaft speed. A similar approach is considered in Bakkeheim et al. (2006), but instead the anti-spin controller is based on a standard shaft speed PI-controller, where the integrator value is reset if appropriate. A Lyapunov function is used to decide when such a reset is suitable. This strategy will only affect the performance in the transient regimes, by speeding up the the controller response only when large control errors are measured, see Bakkeheim and Johansen (2006) and Kalkkuhl et al. (2001) for other applications using this strategy.

In both Smogeli et al. (2004) and Bakkeheim et al. (2006) only DP vessel operations are considered. Extensions of the approach in Smogeli et al. (2004) to transit are given in Smogeli (2006). In this paper a similar approach as in Bakkeheim et al. (2006) is utilized, also covering transit operation, where the vessel speed is larger than in DP. In transit operations, losses due to nonzero advance speed (the speed of the inlet water to the propeller disc) introduces control errors in the actual propeller thrust when using a static mapping from the desired thrust to the desired shaft speed as in Bakkeheim et al. (2006). In Pivano et al. (2007) a dynamic mapping from the desired thrust to the desired shaft speed is presented, compensating for losses due

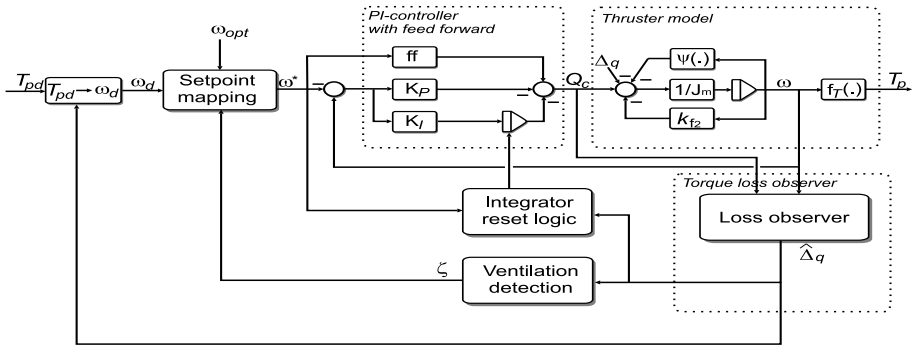

Fig. 1. Local thruster control system.

to nonzero advance speed. By combining the dynamic mapping in Pivano et al. (2007) with the integrator resetting strategy in Bakkeheim et al. (2006), we get an anti-spin controller suitable also for transit operations.

Experimental test results are included in order to demonstrate the performance of this strategy.

2. LOCAL THRUSTER CONTROLLER

An illustration of a local thruster shaft speed control system is given in Figure 1. From the high-level control module, the desired propeller thrust T_{pd} is given as an input to the controller. Further, a reference generator, accounting for losses due to nonzero advance speed, maps the desired thrust into the desired shaft speed ω_d. This is in turn fed into a set-point mapping, limiting the value of the desired shaft speed to some optimal value ω_{opt} when ventilation is detected. A PI-controller with feed-forward from the desired shaft speed gives the commanded torque Q_c to the motor driving the propeller shaft. The main idea in this paper is that the integrator state in the PI-controller may be instantaneously reset to a different value, if appropriate. Consequently, the propeller shaft speed may track the desired one given by the reference generator more accurately.

2.1 Propeller Model

The propeller model to be considered is given by a first-order dynamic system

$$J_m\dot{\omega} = Q_c - \psi(\omega) - k_{f_2}\omega - \Delta_q \tag{1}$$

$$\dot{\Delta}_q = 0 \tag{2}$$

where ω is propeller shaft speed, J_m is shaft moment of inertia and Q_c is commanded torque to the motor drive. This model assumes the dynamics of the electrical part to be negligible when compared to the shaft dynamics. All the nonlinearities are included in the function

$$\psi(\omega) = G_Q|\omega|\omega + k_{f_1}\arctan\left(\frac{\omega}{\epsilon}\right) + k_{f_3}\arctan\left(k_{f_4}\omega\right) \tag{3}$$

where the first term is the nominal propeller torque at zero advance speed in normal conditions, where

$$G_Q = \begin{cases} G_{Q_+}, & \omega \geq 0 \\ G_{Q_-}, & \omega < 0. \end{cases} \tag{4}$$

The constants G_{Q_+} and G_{Q_-} are positive and in general different since the propeller usually is not symmetric with respect to the shaft speed ω. Further, k_{f_i} and ϵ are constant and positive, included in order to model the system friction torque, see Pivano et al. (2007) for more details.

The purpose of Δ_q is to model unknown torque losses due to variations in the vessel speed, propeller submergence, cross flows etc.

Remark 1. It is assumed that Δ_q is constant. This is a simplification. In reality Δ_q varies slowly due to the changes in advance speed, and quickly, almost discrete, due to losses caused by ventilation and in-and-out-of water effects. The controller state reset procedure proposed in this paper makes use of an estimate of Δ_q. This estimate $\hat{\Delta}_q$ triggers the reset procedure only by sudden changes in $\hat{\Delta}_q$. During transients caused by such an incident, we may assume Δ_q being constant due to slowly varying advance speed dynamics.

2.2 Dynamic Controller

Assume ω_d is a smooth and bounded reference, the controller is given as

$$\begin{aligned} Q_c =& J_m\dot{\omega}_d + \psi(\omega_d) + k_{f_2}\omega_d - z - k_P\left(\omega - \omega_d\right) \\ \dot{z} =& k_I\left(\omega - \omega_d\right) \end{aligned} \tag{5}$$

including a feed forward part from ω_d and a regular PI-controller part on the error $\omega - \omega_d$, where $k_P > 0$ and $k_I > 0$ are the proportional and integral gains, respectively. The integrator state z can be interpreted as an estimate for $-\Delta_q$, used in the feed forward compensation in (5), hence similar to the adaptive case. The two states z and ω are stacked into the vector $x = [x_1,\, x_2]^T$, where $x_1 = z$ and $x_2 = \omega$.

The closed-loop error states are defined as $\tilde{x}_1 = z + \Delta_q$ and $\tilde{x}_2 = \omega - \omega_d$, hence from (1) and (5) the error system becomes

$$\dot{\tilde{x}}_1 = k_I\tilde{x}_2 \tag{6a}$$

$$\dot{\tilde{x}}_2 = \frac{1}{J_m}\left(-\left(k_{f_2} + k_P\right)\tilde{x}_2 - g(\tilde{x}_2, \omega_d) - \tilde{x}_1\right) \tag{6b}$$

where the nonlinear function $g(\tilde{x}_2, \omega_d) = \psi(\tilde{x}_2 + \omega_d) - \psi(\omega_d)$ is nondecreasing and inside the sector $[0, \infty]$ in the variable $\tilde{x}_2$, for any fixed ω_d.

2.3 Lyapunov function

A Lyapunov function is used both in order to prove the closed-loop system to be stable and as a measure of the remaining transient "energy", used in the reset procedure.

Lemma 1. The following Lyapunov function proves the origin of the error system (6) to be uniformly globally stable (UGS) and convergent:

$$V = \frac{1}{2}p_{11}\tilde{x}_1^2 + \frac{1}{2}p_{22}\tilde{x}_2^2 \tag{7}$$

where p_{11} and p_{22} are two positive constants, selected such that

$$p_{11} = \frac{p_{22}}{k_I J_m}. \tag{8}$$

Proof: The time derivative of (7) along the trajectories of (6) becomes

$$\begin{aligned}\dot{V} &= p_{11}k_I\tilde{x}_1\tilde{x}_2 \\ &+ \frac{p_{22}}{J_m}\tilde{x}_2\left[-\left(k_{f_2}+k_P\right)\tilde{x}_2 - \tilde{x}_1 - g(\tilde{x}_2,\omega_d)\right].\end{aligned} \tag{9}$$

Using the fact that $g(\tilde{x}_2,\omega_d)\tilde{x}_2 \geq 0\,\forall\omega_d$, $\tilde{x}_2$, and selecting p_{11} as in (8), (9) becomes

$$\dot{V} \leq -\frac{p_{22}}{J_m}\left(k_{f_2}+k_P\right)\tilde{x}_2^2 \tag{10}$$

hence the origin of (6) is UGS. Since $V \geq 0$ is bounded and non-increasing in time we have that $\lim_{t\to\infty}V(\tilde{x}(t)) = V_\infty$ exists and

$$\begin{aligned}\int_0^\infty K\tilde{x}_2^2(\tau)d\tau &= K\int_0^\infty \tilde{x}_2^2(\tau)d\tau \\ &\leq -\int_0^\infty \dot{V}(\tau)d\tau = V_0 - V_\infty\end{aligned} \tag{11}$$

where $K = \frac{p_{22}}{J_m}\left(k_{f_2}+k_P\right)$ and $V_0 = V(\tilde{x}(0))$. The expression in (11) implies that $\tilde{x}_2 \in \mathcal{L}_2$. Since $\omega_d \in \mathcal{L}_\infty$ and $\tilde{x}_1$, $\tilde{x}_2 \in \mathcal{L}_\infty$, due to UGS of the origin (6), from (6b) also $\dot{\tilde{x}}_2 \in \mathcal{L}_\infty$. These conditions imply that $\lim_{t\to\infty}\tilde{x}_2(t) = 0$ from Barbalat's lemma, see Khalil (2001). Further, using the fact that $g(\cdot,\cdot)$ is differentiable and $\dot{\omega}_d \in \mathcal{L}_\infty$, from (6b) $J_m\ddot{\tilde{x}}_2 = -\left(k_{f_2}+k_P\right)\dot{\tilde{x}}_2 - \frac{\partial g}{\partial\tilde{x}_2}(\tilde{x}_2,\omega_d)\dot{\tilde{x}}_2 - \frac{\partial g}{\partial\omega_d}(\tilde{x}_2,\omega_d)\dot{\omega}_d - k_I\tilde{x}_2$ leading to $\ddot{\tilde{x}}_2 \in \mathcal{L}_\infty$, hence $\dot{\tilde{x}}_2$ being Uniformly Continuous (UC). Next, we know that $\int_0^\infty \dot{\tilde{x}}_2(\tau)d\tau = \tilde{x}_2(\infty) - \tilde{x}_2(0)$ exists and is finite, and in combination with $\dot{\tilde{x}}_2$ being UC, $\dot{\tilde{x}}_2(t) \to 0$ as $t \to \infty$ using Barbalat's lemma. From (6b) we conclude that also $\lim_{t\to\infty}\tilde{x}_1(t) = 0$, hence the origin of the error system (6) is convergent.■

Remark 2. If ω_d is constant, the origin of (6) will be globally asymptotically stable (GAS).

2.4 Propeller Torque Loss Observer

The need for an observer estimating the torque losses Δ_q is twofold; one for applying the controller state resetting procedure described in Bakkeheim et al. (2006), and another to include Δ_q in the reference generator developed in Pivano et al. (2007).

A nonlinear observer with gain l_1 and l_2 is designed in order to estimate the torque loss $\hat{\Delta}_q$ and the shaft speed $\hat{\omega} = \hat{y}$:

$$\begin{aligned}J_m\dot{\hat{\omega}} &= Q_c - \psi(\hat{\omega}) - k_{f_2}\hat{\omega} - \hat{\Delta}_q + l_1\left(y-\hat{y}\right) \\ \dot{\hat{\Delta}}_q &= l_2\left(y-\hat{y}\right) \\ y &= \omega\end{aligned} \tag{12}$$

Defining the observer error variables as $\tilde{\omega} = \omega - \hat{\omega}$ and $\tilde{\Delta}_q = \Delta_q - \hat{\Delta}_q$, the observer error dynamics becomes

$$J_m\dot{\tilde{\omega}} = -\left(\psi(\omega) - \psi(\hat{\omega})\right) - l_1\tilde{\omega} - k_{f_2}\tilde{\omega} - \tilde{\Delta}_q \tag{13}$$

$$\dot{\tilde{\Delta}}_q = -l_2\tilde{\omega}. \tag{14}$$

Lemma 2. If the gains l_1 and l_2 are chosen such that

$$\begin{aligned}&A1 \quad l_1 > -k_{f_2} \\ &A2 \quad l_2 < 0\end{aligned} \tag{15}$$

then the origin of (13)-(14) is UGS and convergent.
Proof: Consider the following Lyapunov function for the observer error dynamics (13)-(14)

$$V_o = \frac{1}{2}a_{11}\tilde{\omega}^2 + \frac{1}{2}\tilde{\Delta}_q^2 \tag{16}$$

where $a_{11} = -J_m l_2$ a positive constant. The time derivative of (16) along the trajectories of (13)-(14) is

$$\dot{V}_o = l_2\left(\psi(\omega) - \psi(\hat{\omega})\right)\tilde{\omega} + l_2\left(k_{f_2}+l_1\right)\tilde{\omega}^2. \tag{17}$$

Furthermore, the function $\psi(\cdot)$ belongs to the sector $[0,\,\infty]$ and is non-decreasing, hence $\forall\omega,\,\hat{\omega}\quad[\psi(\omega) - \psi(\hat{\omega})]\left(\omega-\hat{\omega}\right) \geq 0$, hence $\dot{V}_o \leq l_2\left(k_{f_2}+l_1\right)\tilde{\omega}^2$ being negative semi-definite. Using the same argument as in the proof of Lemma 1, (16) will prove the origin of the error system (13)-(14) UGS and convergent.■

The estimates $\hat{\omega}$ and $\hat{\Delta}_q$ can be used to compute an estimate of the propeller torque from

$$\hat{Q}_p = G_Q|\hat{\omega}|\hat{\omega} + \hat{\Delta}_q. \tag{18}$$

2.5 Reference generator

Since the reference is usually given as desired propeller thrust T_{p_d}, a reference generator mapping T_{p_d} to the desired propeller speed ω_d is needed. In Pivano et al. (2007) such a reference generator is proposed. The reference generator is based on the propeller characteristics, usually in the form of the non-dimensional thrust and torque coefficients K_T and K_Q, given as a function of the advance number

$$J = \frac{2\pi u_a}{\omega D} \tag{19}$$

where D is propeller diameter and u_a is the advance speed. The coefficients K_T and K_Q are computed as

$$K_T = \frac{4\pi^2 T_p}{\rho|\omega|\omega D^4} \tag{20}$$

$$K_Q = \frac{4\pi^2 Q_p}{\rho|\omega|\omega D^5}. \tag{21}$$

The proposed reference generator is divided into three main parts. The first part maps T_{p_d} into the desired propeller torque

$$Q_{p_d} = \frac{1}{\hat{G}_{QT(\hat{J})}}T_{p_d} \tag{22}$$

where

$$\hat{G}_{QT(\hat{J})} = \frac{K_T|_{\hat{J}}}{DK_Q|_{\hat{J}}} \tag{23}$$

is an estimate of the actual thrust-torque ratio. An estimate of the advance number $\hat{J}$ is used instead of the real value J, because the advance speed u_a is not

available in practise, see Pivano et al. (2007) for more details.

The second part maps Q_{p_d} into $\bar{\omega}_d$:

$$\bar{\omega}_d = \sqrt{\frac{\left|Q_{p_d} - \hat{\Delta}_q\right|}{G_Q}} \text{sign}(Q_{p_d} - \hat{\Delta}_q). \tag{24}$$

The final part is a second order low pass filter that generates smooth reference signals ω_d and $\dot{\omega}_d$:

$$\ddot{\omega}_d + 2\omega_c\xi\dot{\omega}_d + \omega_c^2\omega_d = \omega_c^2\bar{\omega}_d \tag{25}$$

where ω_c is the cutoff frequency and ξ is relative damping factor.

2.6 Reset procedure

Resetting of the integrator state z to a properly chosen different value z_i may improve the transient performance of the proposed controller in (5), see Bakkeheim et al. (2006).

Lemma 3. A reset of the integrator value $z(t^+)$ to z_i, where t^+ denotes an infinitely small time increment of t, of the system in (6) leads to a jump in the Lyapunov function (7) as follows:

$$\Delta V_i(t) = \frac{p_{11}}{2}\left(z_i^2 + 2\Delta_q\left(z_i - z(t)\right) - z^2(t)\right). \tag{26}$$

Proof: Let $\tilde{x}_{1i} = z_i + \Delta_q$. The jump in the Lyapunov function becoms

$$\begin{aligned}\Delta V_i(t) &= V(\tilde{x}_{1i}, \tilde{x}_2(t^+)) - V(\tilde{x}_1(t), \tilde{x}_2(t)) \\ &= \frac{p_{11}}{2}\left(\left(z_i + \Delta_q\right)^2 - \left(z(t) + \Delta_q\right)^2\right) \\ &= \frac{p_{11}}{2}\left(z_i^2 + 2\Delta_q\left(z_i - z(t)\right) - z^2(t)\right)\end{aligned} \tag{27}$$

where the fact that $\tilde{x}_2(t^+) = \tilde{x}_2(t)$, due to the continuity of solutions of ordinary differential equations, has been used.■

We assume a finite set of integrator reset candidates, $\mathcal{H} = \{z_1, \ldots, z_n\}$. The following result states stability when the integrator is reset.

Proposition 1. Given a closed-loop system with a PI-controller as in (1) and (5). Assume that $V(\tilde{x})$ in (7) is a Lyapunov function that proves the equilibrium point of the nonlinear system in (6) to be UGS and convergent. Further assume that $\Delta V_i(t)$ denotes the jump in the Lyapunov function value if the integrator of the PI-controller in (5) is reset to a different value $z_i \in \mathcal{H}$. Then if $z(t)$ is reset to the value z_i only if $\Delta V_i(t) < 0$, the equilibrium point of the nonlinear system in (6) is UGS and convergent.

Proof: See Bakkeheim et al. (2006).■

Note that Δ_q in (26) is unknown. Instead the estimate $\hat{\Delta}_q$ in (12) is used in the implementation of the reset algorithm. Analyzing the effect of noise in calculation of (26) is neglected. However, in order to reduce erroneous resets and scattering effects due to this issue, a positive threshold δ is added in the resetting procedure. The criterion for performing reset then becomes $\Delta V_i(t) + \delta < 0$.

2.7 Ventilation detection

An estimate of the torque loss factor β_Q is calculated based on the estimated propeller load torque $\hat{Q}_p$ from (18) and the nominal load torque Q_n:

$$\hat{\beta}_Q = \alpha_b(\omega) + (1 - \alpha_b(\omega))\frac{\hat{Q}_p}{Q_n}. \tag{28}$$

where $\alpha_b(\omega)$ is a weighting function of the type

$$\alpha_b(y) = e^{-k|py|^r}. \tag{29}$$

k, p and r are positive tuning gains, needed because the estimate otherwise would be singular for zero shaft speed. The nominal torque, i.e. in case of no ventilation, is computed from the K_Q coefficient through (21) as

$$Q_n = K_Q\frac{\rho|\omega|\omega D^5}{4\pi^2}. \tag{30}$$

The nominal value of K_Q in (30) is derived from the K_Q characteristic where the nominal value of J is computed from (19) using the steady-state relation

$$u_a = (1 - w_f)\, u \tag{31}$$

where $0 < w_f < 1$ is the wake fraction number, often identified from experimental tests, and u is the vessel speed. The wake fraction number accounts for the reduction of water velocity to the propeller caused by the vessel hull.

The estimated loss factor $\hat{\beta}_Q$ may be subject to some fluctuations during the period of ventilation. Instead of using this estimate directly as a measure of whether the propeller is ventilating or not, a translation of this value into a discrete value ζ may be appropriate, as in Smogeli et al. (2004). For a single ventilation incident, ζ will have the following evolution:

$$\begin{aligned}&\hat{\beta}_Q \geq \beta_{v,on} \Rightarrow \zeta = 0 \quad \text{(no ventilation)} \\ &\hat{\beta}_Q < \beta_{v,on} \Rightarrow \zeta = 1 \quad \text{(ventilation)} \\ &\hat{\beta}_Q \geq \beta_{v,off} \Rightarrow \zeta = 0 \quad \text{(no ventilation)}.\end{aligned} \tag{32}$$

Note that the ventilation detection ζ includes hysteresis, hence robustness due to measurement noise in the loss value estimate $\hat{\beta}_Q$ is achieved.

2.8 Set-point mapping

The reference generator (24), designed to counteract the losses due to nonzero advance speed, fails when ventilation occurs. This is so because losses due to ventilation are not accounted for. Anti-spin set-point mapping is used in order to reduce the shaft speed reference in case of ventilation

$$\omega^* = \begin{cases} \omega_{opt}, & \text{if } \zeta = 1 \text{ and } \omega_d \geq \omega_{opt} \\ \omega_d, & \text{otherwise} \end{cases} \tag{33}$$

where ω_{opt} is some optimal propeller shaft speed during ventilation, see Smogeli (2006) for models used to compute ω_{opt}.

3. EXPERIMENTAL TEST RESULTS

A thruster set-up with propeller disc diameter $D = 0.25m$ and shaft moment of inertia $J_m = 0.006kgms^2$ was used to experimentally test the proposed strategy in the Marine Cybernetics Laboratory (MCLab) at NTNU.

The tuning of the overall controller was performed in several steps. The friction parameters k_{f_i} and ϵ were

identified by running the propeller in free air at different speeds ω. The parameters for the PI-controller were found by focusing on the control performance in calm and moderate seas. The resulting parameters led to a relatively slow controller response, where the commanded torque Q_c avoids wear and tear on the mechanical components. Next, the loss observer and reference generator were tuned in order to operate in calm sea conditions. Further, the ventilation detection with set-point mapping was tuned in order to handle extreme sea situations. Finally, the parameters of the reset procedure was tuned in extreme sea conditions.

The resulting parameters for the PI-controller was $k_P = 0.07$ and $k_I = 0.8$. The observer parameters were selected to be $l_1 = 3.2$, satisfying **A1** in Lemma 2, and $l_2 = -160$, satisfying **A2** in Lemma 2. The optimal controller speed during ventilation was selected to be $\omega_{opt_+} = 45$ and $\omega_{opt_-} = 54$ for positive and negative shaft speed, respectively. The Lyapunov function coefficients were selected to be $p_{11} = 21$ and $p_{22} = 0.1$, hence satisfying (8). The tuning of the resetting procedure was then restricted to select a suitable δ in order to yield acceptable performance. $\delta = 100$ turned out to work fine. The reset candidates $\mathcal{H} = \{z_1, \ldots, z_n\}$ both need to span the working area of the integrator state z and to address robustness properties for the reset procedure by appropriately selection of candidate sparseness. $\mathcal{H} = \{-6.6, -4.4, -2.2, 0, 2.2, 4.4, 6.6\}$ gave satisfactory performance.

A thruster mounted on a moving towing carriage was employed in order to demonstrate the strategy. Extreme seas conditions were simulated by raising and lowering the thruster into the water with a period of $6.6s$ and amplitude of $15cm$. This way of emulating waves gives total control of the environmental interaction with the thruster setup. This leads to a more accurate way of comparing different controller algorithms.

Figures 2 and 3 show data from the test without and with resetting the integrator state, respectively. The thruster vertical position was moved in order to trigger ventilation and in-and-out of water effects, presented as relative submergence h/R, where $R = D/2$ is the propeller radius and h is the submergence of the propeller shaft. The time series of σ shows integrator reset incidents. When σ is nonzero, say $\sigma = i$, a reset to candidate $z_i \in \mathcal{H}$ is performed. Motor power P_m is included in order to show power fluctuations generating power peaks on the power network.

The test scenario was the same for both cases. The commanded thrust T_{pd} had the pattern seen in Figure 2(b), with amplitude $120N$. The emulated resulting speed of the towing carriage u had an amplitude $0.7m/s$, dephased from the commanded thrust. The combination of the behavior of T_{pd} and u yields operation in 4 quadrants. In this case, $u_a = u$.

In Figure 2 the controller is tuned for operating in calm sea. As seen in Figure 2(b), the propeller speed increases when the propeller rotates close to the water surface. These peaks in rotational speed are reduced when the integrator reset is made active, see Figure 3(b). Also note the reduction in power peaks, hence reducing the risk of blackouts due to fluctuations on the electric power network. Despite this reductions in power peaks, the average thrust production is kept more or less constant.

4. CONCLUSIONS

An integrator reset strategy for a PI shaft speed thruster controller has been presented. A Lyapunov function is used to decide when to reset and to prove asymptotic stability of the overall system. A dynamic reference generator is included in order to increase the performance when a ship is in transit operation.

In order to emulate operation in 4 quadrants and extreme seas conditions, the propeller was towed through the water and at the same time moved along its vertical axis. Tests showed reduced peaks in propeller speed, hence reduction of structural loads on propeller blades, while not changing the mean propeller thrust significantly. Reduction of power peaks was also achieved, hence reduced risk of blackouts due to fluctuations on the electric power network.

5. ACKNOWLEDGEMENTS

This work was in part sponsored by the Research Council of Norway, project number 157805/V30.

REFERENCES

J. Bakkeheim and T. A. Johansen. Transient Performance, Estimator Resetting and Filtering in Nonlinear Multiple Model Adaptive Backstepping Control. *IEE Proc.-Control Theory Appl.*, 153:536–545, 2006.

J. Bakkeheim, Ø. N. Smogeli, T. A. Johansen, and A. J. Sørensen. Improved Transient Performance by Lyapunov-based Integrator Reset of PI Thruster Control in Extreme Seas. In *IEEE Conference on Decision and Control*, San Diego, USA, 2006.

J. Kalkkuhl, T. A. Johansen, J. Lüdemann, and A. Queda. Nonlinear Adaptive Backstepping with Estimator Resetting Using Multiple Observers. In *Proc. Workshop on Hybrid Systems, Computation and Control, Rome*, 2001.

H. K. Khalil. *Nonlinear Systems (3rd Ed.)*. Prentice-Hall, New York, 2001.

L. Pivano, T. A. Johansen, Ø. N. Smogeli, and T. I. Fossen. Nonlinear Thrust Controller for Marine Propellers in Four-Quadrant Operations. *to appear at the 26th American Control Conference (ACC07), New York, USA*, July 2007.

D. Radan, Ø. N. Smogeli, A. J. Sørensen, and A. K. Ådnanes. Operating Criteria for Design of Power Management Systems on Ships. In *Proc. of the 7th IFAC Conference on Manoeuvring and Control of Marine Craft (MCMC'06)*, Lisbon, Portugal, 2006.

Ø. N. Smogeli. *Control of Marine Propellers: from Normal to Extreme Conditions*. PhD thesis, Department of Marine Technology, Norwegian University of Science and Technology (NTNU), 2006.

Ø. N. Smogeli, J. Hansen, A. J. Sørensen, and T. A. Johansen. Anti-spin Control for Marine Propulsion Systems. In *IEEE Conference on Decision and Control*, Bahamas, December 2004.

A. J. Sørensen. Structural Issues in the Design and Operation of Marine Control Systems. *IFAC Journal of Annual Reviews in Control*, (29:1):125–149, 2005.

L. L. Whitcomb and D. Yoerger. Developement, Comparison, and Preliminary Experimental Validation of Nonlinear Dynamic Thruster Models. *IEEE Journal of Oceanic Engineering*, 24(4):481–494, Oct. 1999.

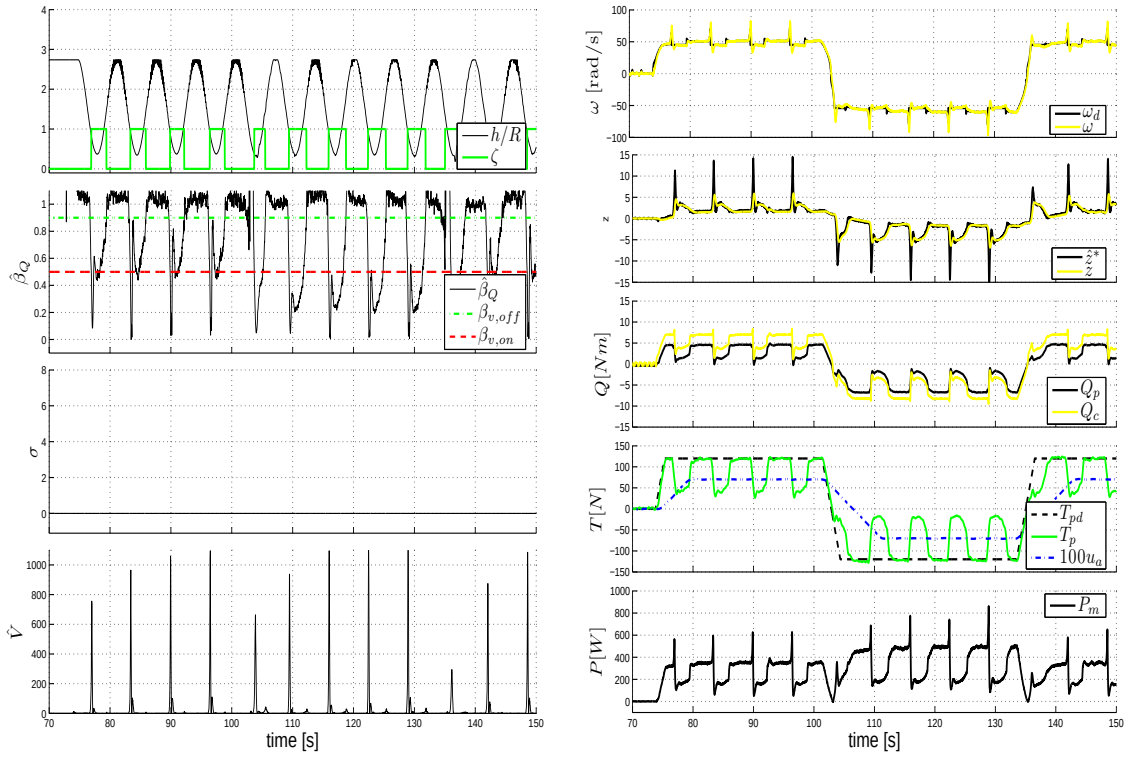

(a) (b)

Fig. 2. Experimental results of shaft speed PI-control without reset. The figure shows in (a) relative submergence h/R, ventilation detection signal ζ, estimated loss value $\hat{\beta}_Q$, reset index value σ and estimated Lyapunov function value $\hat{V}$. And in (b) desired shaft speed ω_d, actual shaft speed ω, estimated integrator value $\hat{z}^*$, actual integrator value z, measured propeller torque Q_p, commanded torque Q_c, desired thrust T_{pd}, measured thrust T_p, propeller advance speed u_a and motor power P_m.

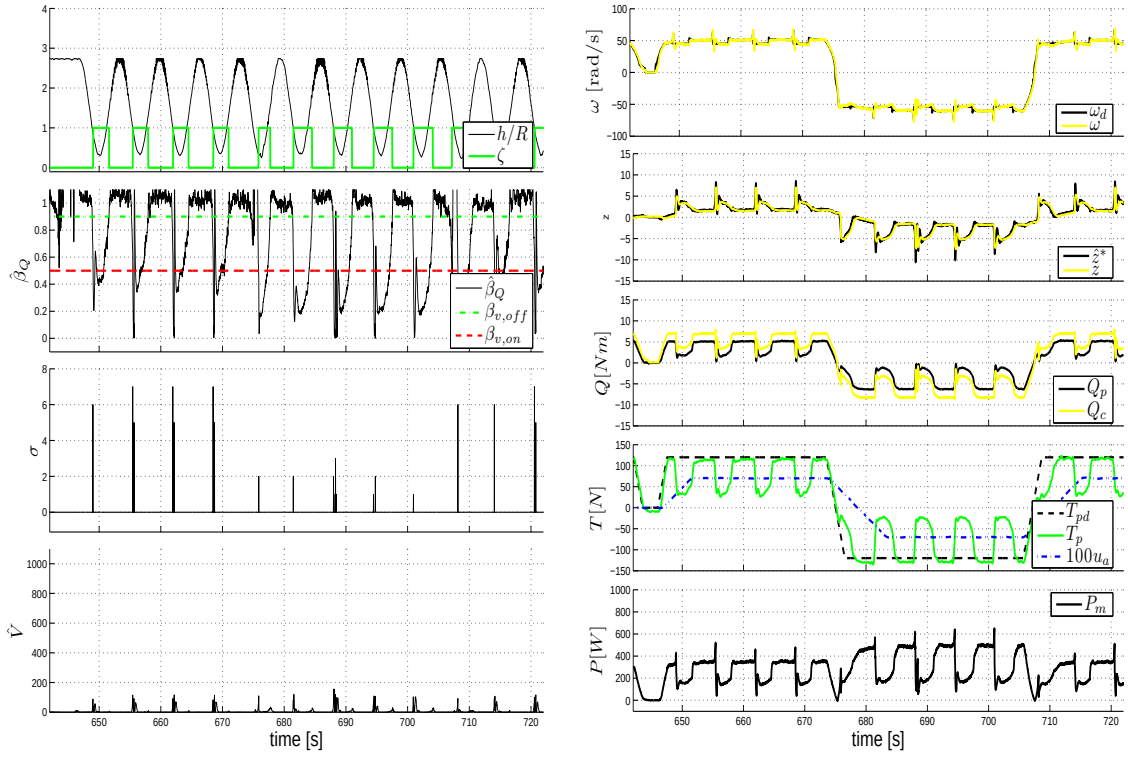

(a) (b)

Fig. 3. Same as Figure 2, but with integrator reset made active.